

Evaluating tephrochronology in the permafrost peatlands of Northern Sweden

Claire L. Cooper^{*1,2}, Graeme T. Swindles^{1,3}, Elizabeth J. Watson¹, Ivan P. Savov², Mariusz Galka⁴, Angela Gallego-Sala⁵, Werner Borken⁶

¹ School of Geography, University of Leeds, UK, LS2 9JT

² School of Earth and Environment, University of Leeds, UK, LS2 9JT

³ Ottawa-Carleton Geoscience Centre and Department of Earth Sciences, Carleton University, Canada

⁴ Dept. of Biogeography and Palaeoecology, Adam Mickiewicz University, Poland

⁵ School of Geography, University of Exeter, UK, EX4 4RJ

⁶ Dept. of Soil Ecology, University of Bayreuth, Germany

* Corresponding author: gyclc@leeds.ac.uk

For submission to: *Quaternary Geochronology*

Keywords: *tephra; peatlands; permafrost; glass preservation; tephrochronology*

23 **Highlights**

- 24 • Six tephra layers are identified in sub-Arctic peatlands at Abisko, Sweden
- 25 • Geochemical analyses of glass shards are presented, identifying material
- 26 belonging to the Hekla 4, Hekla-Selsund, Hekla 1104, and Hekla 1158
- 27 eruptions
- 28 • Variation in the deposition and preservation of tephra layers across adjacent
- 29 profiles is identified and discussed

30

31 **Abstract**

32 Tephrochronology is an increasingly important tool for the dating of sediment and
33 peat profiles for palaeoecological, palaeoclimatic and archaeological research.
34 However, although much work has been done on tephra in temperate peatlands,
35 there have been very few in-depth investigations of permafrost peatlands. Here we
36 present the analysis of nine peatland cores from Abisko, northern Sweden, and show
37 that the presence of tephra layers may be highly variable even over a scale of <10
38 km. Using electron probe microanalysis (EPMA) combined with age-depth profiles
39 compiled from radiocarbon (^{14}C) and ^{210}Pb dating of peat records, we identify the
40 Hekla 1104, Hekla 1158, Hekla-Selsund and the Hekla 4 tephra layers. We also infer
41 the presence of the Askja 1875 tephra, in addition to an unassigned tephra dating
42 from between 1971-1987 AD in two separate cores. Five of the nine analysed cores
43 do not contain distinct tephra layers. Volcanic ash deposits in northern Scandinavia
44 are subject to both regional-scale variations in climate and atmospheric circulation,
45 and local-scale variations on the order of tens of kilometres in topography,
46 vegetation, snow cover, and ground permeability. The extreme inconsistency of

47 tephra preservation within a small study area (~3000 km²) brings into question the
48 reliability of tephrochronology within permafrost peatlands, and highlights the
49 necessity of alternative methods for dating peat profiles in this region.

50

51 **1 Introduction**

52 The study of volcanic ash preserved in peatlands and lake sediments is a well-
53 established science, particularly across western Europe and North America (Lowe,
54 2011; Stivrins et al., 2016; Watson et al., 2016a; Plunkett et al., 2018; Swindles et al.,
55 2018). Light ash particles from volcanic eruptions are carried across continents by
56 atmospheric currents, sometimes being transported thousands of kilometres from
57 their source (Cadle et al., 1976; Palais et al., 1992; Bourne et al., 2016). The fallout
58 from these eruptions may then be preserved in layers in soft sediments such as in
59 peatlands and lakes, providing useful markers and isochrons across multiple sites.
60 Tephra layers linked to particular eruptions allow sediment profiles to be correlated
61 to specific points in time. Assuming that ash deposition occurs approximately
62 simultaneously across multiple sites, applying tephrochronology to a given record
63 allows for precise, high-resolution chronological reconstruction of sediment
64 columns, with a range of environmental and archaeological applications (Lowe et al.,
65 2011; Lane et al., 2014). However, relatively few tephrochronological studies have
66 been performed on permafrost peatlands in Europe compared to temperate
67 peatlands (Watson et al., 2016).

68

69 Abisko Scientific Research Station is located in the Scandinavian Arctic,
70 approximately 30 kilometres north of the polar circle at 68°21' N, 18°49'E. The

71 station has a long history of wide-ranging environmental and ecological research,
72 with many recent studies focusing on the observations and effects of climate change
73 in a boreal environment (Alatalo et al., 2016; Lundin et al., 2016; Lett, 2017). Rapid
74 alterations in the local climate over the past 50 years and an increase in the
75 frequency of winter warming events in northern Scandinavia (Vikhamar-Schuler et
76 al., 2016) have caused significant ecological concern. The warmer conditions have
77 been linked to vast reductions in the extent of permafrost in the area (Osterkamp &
78 Romanovsky, 1999; Camill, 2003; Schuur & Abbott, 2011), affecting the surface
79 water pH, water table depth and vegetation in permafrost peatlands (Camill, 1999).

80

81 Wetlands have long been acknowledged as playing a significant role in global carbon
82 emissions and sequestration (Lai, 2009). It is therefore increasingly important for the
83 scientific community to develop an understanding of how permafrost peatlands in
84 this area have changed over time in terms of their ecology, hydrology and carbon
85 accumulation (Swindles et al., 2015b). Accurate and precise chronological control is a
86 crucial component of such investigations into peat archives.

87

88 Projections of jet stream currents in the northern hemisphere suggest that, under
89 typical atmospheric circulation conditions, ash particles injected into the
90 stratosphere by Icelandic eruptions should be carried and deposited across much of
91 north-western Europe, including Scandinavia (Woollings et al., 2010; Davies et al.,
92 2010). Past studies have borne this assumption out, and Icelandic tephra has been
93 found across the UK, Ireland, France, Germany, Poland, Belgium, Switzerland,
94 Denmark, Sweden, Norway, and the Faroe Islands (Swindles et al., 2011; Lowe et al.,

2011; Watson et al., 2017). However, some disparity between the sediment records of adjacent sites has been noted at several locations (Watson et al., 2016b). Vegetation, local weather at the time of deposition, pH conditions in the sediment, and storm events can all affect the capture and preservation of glass shards (Watson et al., 2016a), resulting in variation across cores, even over distances of a few kilometres. Northern Scandinavia is on the extreme distal edge of most numerical simulations reconstructing Icelandic ash clouds (Davies et al., 2010), making consistent ash fall across wide areas possible, but unlikely. In this paper, we investigate the cryptotephra content (distal tephra <150 µm along the longest axis) of nine cores collected in the vicinity of the Abisko field station. We also discuss the factors affecting shard preservation variability in the area, and consider the implications for future tephrochronological research in this region.

107

108 **2 Materials and Methods**

109 *2.1 Study Area*

110 [Figure 1: Map of study area, showing local topography and the location of coring
111 sites]

112 Nine samples were collected from peatland sites near Abisko, northern Sweden,
113 seen in Figure 1, using a Russian peat corer. Each sample is between 20-45 cm in
114 depth, and is comprised largely of peat, in addition to occasional lenses of organic
115 mud.

116

117 Abisko is located within the rain shadow of the Norwegian mountains, and as such
118 receives a relatively small amount of precipitation (332 mm per year; Callaghan et

119 al., 2010), with the highest rainfall occurring during the summer months. Each of the
120 peatlands sampled were part of peat complexes in various stages of permafrost
121 decomposition, from early dome collapse to full inundation after permafrost thaw.
122 The peatlands of the region are primarily composed of ombotrophic bogs, peat
123 plateaus, arctic fens, and palsa mires, many of which are in states of permafrost
124 collapse as a result of rapid warming. Recent studies have shown an increased rate
125 of permafrost decay in some of the Abisko sites, such as Stordalen (Swindles et al.,
126 2015b)

127

128 *2.2 Methods*

129 Coring locations were selected on the basis of physical features, hydrology, and
130 vegetation composition (Swindles et al., 2015a). Sites were deemed suitable if they
131 were situated on relatively flat ground, and could be characterised as fens, bogs, or
132 palsas. Full site details may be found in appendix C. The cores were stored in plastic
133 wrap and aluminium foil, and kept at a temperature of 4°C prior to analysis.
134 Extraction of the tephra in these sediment samples was performed following the
135 method detailed by De Vleeschouwer et al., 2010. Each peat core was divided into
136 continuous sections of 1cm depth, and a sample of 4 cm³ was removed from each.
137 These samples were weighed and dried in ceramic crucibles at 105°C for a minimum
138 of 12 hours. The dry samples were then reduced to ashes in a muffle furnace at
139 600°C for six hours. After each stage of burning and drying, the samples were
140 weighed to estimate gravimetric water content and mass loss on ignition. These
141 ashes were suspended in 10% hydrochloric acid for 24 hours to remove carbonate
142 material, and then washed with deionised water. The tephra was concentrated at

143 the bottom of the test tubes by placing the aqueous samples in a centrifuge at 3000
144 r.p.m. for approximately five minutes. This aqueous material was then sieved
145 through a 10µm mesh. Petrographic slides were prepared by adding the aqueous
146 solution to a glass slide on a hotplate until the liquid component evaporated. The
147 slides were mounted using Histomount and a glass coverslip, and examined through
148 optical microscopy using 200-400x magnification to assess tephra content.
149 References to several visual and descriptive sources were used to ensure positive
150 tephra identification (Lowe, 2011; Watson et al., 2016a).

151

152 Sub-samples which were found to contain more than 10 shards per cm³ were re-
153 sampled and processed using the acid digestion method outlined in Dugmore &
154 Newton (1992), and, later, to density separation, to fully remove problematic organic
155 material and biogenic silica (Blockley et al., 2005). In some cases, tephra was found
156 to exist in irregular, non-continuous, discrete clumps of material rather than in well-
157 defined layers, making repeated extractions from a particular depth within the peat
158 profile problematic. In these instances, optical slides containing tephra were
159 submerged in a xylene solution for 48 hours to dissolve the mounting agent
160 (Ravikumar et al., 2014). This method was found to be highly effective in retaining
161 the tephra and organic material while completely removing the Histomount. Samples
162 for geochemical analysis were then dried, remounted in blocks of resin and
163 subjected to electron probe microanalysis EPMA at the Tephra Analytical Unit,
164 University of Edinburgh. All analysis was performed using a 5µm diameter beam of
165 15kV with a current of either 2nA (Na, Mg, Al, Si, K, Ca, and Fe) or 80nA (P, Ti, Mn),
166 following the method of Hayward (2012). Lipari and BCR-2G basalt glass standards

167 were used for external calibration (Watson et al., 2015). The standard data
168 generated during geochemical analysis may be found in table B.2 in the appendices.
169 The overall data for the standards returns <1% variability for most major elements.

170

171 Radiocarbon signatures of organic material were determined by accelerator mass
172 spectrometry (AMS). Subsamples of 0.8 mg C were combusted in 6 mm sealed quartz
173 tubes with 60 mg CuO oxidizer and 1 cm silver wire for 2 hours at 900°C. The
174 resulting CO₂ was purified from water and non-condensable compounds. Afterwards,
175 CO₂ was reduced to graphite using the zinc reduction method where TiH₂ and Zn
176 with Fe act as catalysts at 550°C for 7.5 hours (Xu et al., 2007). All preparations took
177 place at the Department of Soil Ecology at the University of Bayreuth. The graphite
178 targets were analysed by the Keck-CCAMS facility of the University of California,
179 Irvine, with a precision of 2–3‰ (‰ deviation is from the ¹⁴C/¹²C ratio of oxalic acid
180 standard in 1950). The samples were corrected to a δ¹³C value of -25‰ to account
181 for any mass dependent fractionation effects (Stuiver & Polach, 1977). Radiocarbon
182 signatures were converted to ¹⁴C age before present (BP) using the IntCal13
183 calibration curve (Reimer et al., 2013). Full radiocarbon dating results may be found
184 in table A.1 in the appendices.

185

186 Further chronological data for the Marooned and Stordalen cores was established
187 through ²¹⁰Pb dating. Peat samples were digested using a combination of
188 concentrated HCl, HNO₃, and H₂O₂. A small amount of ²⁰⁹Po was then added as a
189 tracer. Following the method detailed in Whittle & Gallego-Sala (2016), the material
190 was plated onto silver disks, and alpha spectrometry was performed using an Ortec

191 Octête Plus Integrated Alpha-Spectrometry System at the University of Exeter (UK)
192 Radiometry Lab. ^{210}Pb values were derived from the $^{210}\text{Po}/^{209}\text{Po}$ ratios, and dates
193 were then extrapolated from the ^{210}Pb inventory using the constant rate of supply
194 model (Appleby, 2001).

195

196 **3 Results**

197 *3.1 Tephrostratigraphies*

198 [Figure 2: Tephrostratigraphic profiles of Abisko peat cores. Radiocarbon dates (cal
199 BP) are shown in red along the vertical axes. a) Crater Pool 1; b) Crater Pool 2; c)
200 Eagle Bog; d) Electric Bog; e) Instrument Core; f) Nikka Bog; g) Marooned Bog; h)
201 Railway Bog; i) Stordalen Core]

202 Figure 2 shows the tephra counts per 4 cm^3 of the eight peat profiles collected in
203 Abisko, along with the percentage loss on ignition, and age-depth models based on
204 radiocarbon dating of organic material. While four profiles – Stordalen (ST),
205 Marooned (MN), Eagle (EA), and Nikka (NI) – have clear tephra peaks at varying
206 depths, the other profiles have only minimal volcanic ash content, averaging only 1-3
207 glass shards per section. There is little to no consistency in the presence of tephra
208 with depth across the profiles. The loss-on-ignition for each profile is high, typically
209 between 80 – 90 %, but there is no apparent correlation with the presence of glass.
210 The glass shards themselves were typically between 10-150 μm , though a wide range
211 of morphologies were present, from thin, concave, wisp-like structures to larger
212 aggregate shards. As the shards in EA12 and NI8 were found to be too small and
213 sparse to perform EPMA, ^{210}Pb dating of the profiles containing these layers was
214 used to determine their ages. The major element geochemistry of the glass found in

215 the Marooned and Stordalen cores can be found in figure 4. Full geochemistries and
216 profile dates may be found in the appendices.

217

218 [Figure 3: Age-depth models of Eagle, Nikka, and Stordalen peatland profiles. Tephra
219 profiles identified in this paper are marked in red. Full radiocarbon and ^{210}Pb data
220 can be found in appendix A.]

221

222 3.1.1 MN85/Hekla 4

223 Figure 4 shows the geochemistry of tephra shards found at in the Marooned and
224 Stordalen cores. Shards matching the geochemistry of the Hekla 4 eruption were
225 found at a depth of 85 cm in the Marooned bog core. The Hekla 4 eruption
226 represents the most widespread tephra deposit in northern Europe, and relates to a
227 plinian eruption of Hekla occurring between 2395-2297 BC (Pilcher & Hall, 1996;
228 Watson et al., 2017). Tephra attributed to this deposit occurs across a range of
229 compositions from dacitic to rhyolitic; in the case of the tephra found in Marooned
230 bog, the silica content ranges between 63 – 77 %.

231

232 3.1.2 MN70/Hekla-Selsund

233 The Hekla-Selsund tephra, also known as the Kebister tephra, is dated as occurring
234 between 1800-1750 BC, and can be found in multiple sites across north-western
235 Europe, including Germany, Great Britain, the Faroe Islands and Scandinavia (Watson
236 et al., 2017). In Abisko, it occurs in the Marooned bog core at a depth of 70 cm. This
237 tephra is rhyolitic to dacitic in composition.

238

239 3.1.3 ST30/Hekla 1104 (*Hekla 1*)

240 These glass shards closely match the geochemistry of the Hekla 1104 eruption (also
241 known as the Hekla 1 eruption), with an average SiO₂ content of 63-67%. This tephra
242 has previously been found in multiple sites in northern Scandinavia, including the
243 Sammakovuoma peatland in northern Sweden (Watson et al., 2016a) and the
244 Lofoten Islands in arctic Norway (Pilcher et al., 2005); see figure 5.

245

246 3.1.4 ST25/Hekla 1158

247 Several shards with geochemistries similar to Hekla 1158 were found in the
248 Stordalen core at a depth of 23 cm. Tephra from the Hekla 1158 eruption is dacitic in
249 composition, with a silica content of 67-68%. Evidence of this eruption has only
250 recently been found in Europe, in Scandinavian sites in almost all instances (Pilcher
251 et al., 2005; Swindles et al., 2015a).

252

253 3.1.5 EA12/Askja 1875

254 Using the combined age-depth profile (figure 3), it can be seen that the layer in EA
255 falls approximately between 1831 and 1920. A likely candidate for this tephra is
256 therefore the Askja 1875 eruption. Ash from this eruption has previously been found
257 in several sites in Scandinavia (Pilcher et al., 2005; Wastegård, 2008; Watson et al.,
258 2016b), suggesting that the tephra cloud was at least partially carried in a north-
259 easterly heading from the source (the Dyngjufjöll volcanic system). Approximately
260 0.5 km³ of rhyolitic tephra was produced during this eruption (Sigurdsson & Sparks,
261 1981).

262

263 3.1.6 NI5 (*Unknown tephra*)

264 Using our precise ^{210}Pb chronology, the layer in NI appears to fall between 1971 and
265 1987, and is therefore of a more uncertain origin as no tephra layers from this period
266 have yet been defined in Scandinavia at the time of writing. As stated above, it was
267 not possible to perform geochemical analysis on these shards; however, several
268 potential source eruptions occurred in Iceland during this period. The Hekla and
269 Krafla volcanic systems both exhibited significant activity, although no tephra from
270 the eruptions occurring at Hekla in 1980 and 1981 has yet been reported outside
271 Iceland. The activity from Krafla was almost exclusively effusive with intermittent
272 phreatic explosions (Global Volcanism Program, 2013), making this an unlikely
273 candidate for distal tephra deposition. A minor subglacial eruption of Grímsvötn
274 occurred in 1983, though again this is unlikely to have produced a sufficient tephra
275 cloud to account for the reported layer (Gronvold & Johannesson, 1984). It is
276 therefore possible that this tephra originated from a non-Icelandic source. Tephra
277 attributed to Alaskan volcanoes has previously been found in northern Scandinavia
278 (Watson et al., 2017), and it has recently been suggested that a previously
279 unidentified tephra found in Svartkälsjärn, Sweden (Watson et al., 2016a) may have
280 originated from the Cascades arc in North America (Plunkett & Pilcher, 2018). These
281 findings indicate that, while Iceland is statistically the most likely source of volcanic
282 ash in Scandinavian peatlands, it may be necessary to look further afield to identify
283 more obscure deposits.

284

285 [Figure 4: Geochemical bi-plots of glass shards found in the Marooned and Stordalen
286 cores, showing the geochemical type-data envelopes of the eruptions to which they

287 correlate. Also shown are geochemical envelopes for alternative eruptions occurring
288 within a similar timeframe for comparison. a) ST25, b) ST30, c) MN70, d) MN85.
289 EPMA was performed at the Tephra Analysis Unit, University of Edinburgh.]

290

291 **4 Discussion**

292 *4.1 Tephra transport and preservation*

293 [Figure 5: Spatial distributions within Europe of four tephra layers found in the
294 Abisko peatlands. All four originated at Hekla in southern Iceland, and each has
295 previously been found within Scandinavia. (Swindles et al., 2017)]

296

297 While several distinct deposits of tephra were found within the Abisko region, there
298 is poor correlation of tephra preservation across sites, even between cores
299 separated by <10 km. A distinct tephra layer can clearly be found in the Eagle bog
300 site, but is not present at the Craterpool bog, despite the two locations being within
301 12 km of each other. The same is true of the Marooned and Railway bog sites, which
302 are 9 km apart.

303 There are a number of components influencing the spatial distribution of tephra over
304 a given deposition area. 'Ash winnowing', referring to the resorting and redeposition
305 of ash sediments, is a phenomenon which has been previously noted in many
306 volcanological studies, and is typically attributed to erosion by wind- or water-based
307 processes. Analysis of distal ash deposits from the 2008 eruption of Chaitén, Chile,
308 for example, showed that unsheltered locations occasionally displayed greater
309 degrees of reworking and variability in deposit thickness, and that these anomalies
310 became more frequent with distance from the eruption source (Watt et al., 2009).

311 The disparities across the stratigraphic columns shown in our results emphasise how
312 a combination of components can cause extreme variability in glass preservation,
313 even over a relatively small area. Many factors are related to local conditions at the
314 time of deposition, while others relate to broader factors such as regional
315 topography and basin drainage systems. Additionally, eruption conditions at the
316 origin volcano can affect glass composition and ash shard morphology, with
317 implications for tephra preservation and transport respectively (Lowe, 2011). Figure
318 6 provides a summary of the dominant factors, some of which are explained in
319 greater detail below.

320

321 4.2 *Site analysis*

322 [Figure 6: Conceptual diagram of factors influencing tephra preservation in Abisko
323 peatlands.]

324

325 4.2.1 *Local climate and wind currents*

326 The location of Abisko on the leeward side of the Norwegian mountains results in a
327 significant decline in annual rainfall relative to nearby locations on the windward
328 side (Swindles et al., 2015b). While this may decrease the surface runoff in the
329 region, thus decreasing the likelihood of surface redistribution of fallen tephra, it is
330 also thought that precipitation itself may play a crucial role in the deposition of
331 tephra (Davies et al., 2010). Some studies attribute the patchiness of the Hekla 1947
332 tephra in many areas of Europe to irregular rain- or snowfall (Salmi, 1948;
333 Thorarinsson, 1967).

334

335 Another factor to consider when assessing the impact of precipitation on ash
336 preservation is snow cover. Snow provides a 'shielding' layer above the underlying
337 peatland, enabling redistribution of deposited tephra through surface wind currents
338 (Bergman et al., 2004). Tephra preserved within snow is also subject to
339 transportation should that snow cover melt during seasonal temperature changes.

340

341 The variability of air currents over northern Scandinavia is also likely to be a major
342 controlling factor on tephra deposition in the region. Models suggest that seasonal
343 variability in the dominant air currents has a strong influence on tephra
344 transportation, with strong westerlies at high elevations (>15 km) during autumn and
345 winter, and weak easterlies becoming dominant during spring and summer (Lacasse,
346 2001). Icelandic eruptions occurring during the latter half of a given year
347 (September-February) are therefore more likely to deposit tephra across
348 Scandinavia. In recent years, however, evidence has emerged that the Earth's
349 warming climate may have a weakening effect on the polar vortex (Kim et al., 2014).
350 If this is proved to be the case, future patterns of tephra distribution in the northern
351 hemisphere may be altered by continuing climate change.

352

353 Additionally, it has been suggested that, under the correct conditions, the
354 combination of a variable wind field and changes to the eruption parameters due to
355 fluctuations in the volcanic system may allow for the creation of discrete deposition
356 patterns for different phases of an eruption (Watt et al., 2009; Stevenson et al.,
357 2012). This may provide an explanation for the unusually uniform major element
358 geochemistries seen in some of the deposits found in Abisko, most notably the ST25

359 and ST30 deposits, attributed to Hekla 1158 and Hekla 1104 respectively. These
360 shard clusters may represent ashfall from a particular phase of those eruptions,
361 though whether the compositional bias in these deposits occurred during transport
362 or through winnowing and preservation processes is unclear.

363

364 Studies of ashfall conducted following the 2008 eruption of Chaitén, Chile indicate a
365 complex pattern of ash deposition which was largely attributed to variable wind
366 fields during the course of the week-long eruption, at least on a proximal scale (Watt
367 et al., 2009; Alfano et al., 2010; Durant et al., 2012). However, variations in wind
368 patterns are typically referenced as a cause of regional-scale depositional variations
369 on the order of hundreds of kilometres, as opposed to the local-scale variations
370 observed in Abisko, which occur across areas of <20 km. While a variable wind field
371 therefore offers a potential explanation for the apparent underrepresentation of
372 many historical Icelandic tephra deposits in Scandinavia relative to the rest of
373 western mainland Europe, shifting regional air currents are unlikely to have caused
374 the erratic preservation pattern observed at Abisko.

375

376 4.2.2 Vegetation

377 Similarly to snow cover, vegetation can provide a shielding effect to underlying
378 sediment. However, a more significant implication for tephra preservation is the
379 effect of root trapping, wherein plant roots capture small packets of sediment,
380 preserving them at a given depth. This has multiple negative consequences for the
381 field of tephrochronology; firstly, the unequal distribution of ash within a given
382 horizon complicates the process of tephra extraction, as it makes the presence of a

particular layer at a given depth more uncertain. Additionally, the vertical redistribution of tephra can negatively impact the creation of age-depth profiles for peatlands and lake sediment, as the correlation between tephra layers and dated organic material from the same layer becomes less reliable (Cutler et al., 2016). Dugmore et al., 2018, suggest that uniformly vegetated slopes can produce consistent tephra layers in the stratigraphic record, but areas of sparse or patchy vegetation will result in variability. Many of the Abisko sites were characterised by a uniform top layer of sphagnum moss of between 1-4cm thickness, with intermittent tussocks of thicker vegetation and herbaceous plants such as cotton sedge (*Eriophorum angustifolium*). Studies of vegetation succession in the Marooned and Stordalen sites also indicate the variable presence of shrub communities over the past millennium (Gałka et al., 2017), making it likely that root trapping could have interfered with tephra preservation in this region.

Ashfall may also be intercepted by vegetation at a sub-aerial level, such as on leaves and branches. However, the sparseness of larger forms of plant life in most sub-Arctic peatland reduces the influence of this factor in this region.

399

400 4.2.3 Topography

A recent study (Dugmore et al., 2018) based on data from Iceland and Washington State, USA, has shown that tephra layers of 1-10 cm thickness can remain stable on slopes $<35^\circ$, given sufficiently uniform vegetation cover. Slopes of a greater angle are unlikely to produce consistent stratigraphic records, as tephra particles become concentrated in topographic hollows, resulting in down-slope thickening which can cause differences in thickness as great as an order of magnitude between the peak

407 and the base of a slope (Mairs et al., 2006). Down-slope runoff processes can be
408 mitigated by vegetation and ground cover, resulting in small-scale variation within a
409 given layer.

410

411 *4.2.4 Eruption conditions*

412 Eruption conditions represent a strong control on cryptotephra layers. Very fine ash
413 of the size and density suitable for airborne transport over several thousand
414 kilometres is generated in far greater quantities during explosive silicic eruptions
415 than effusive basaltic eruptions (Rose & Durant, 2009). The effects of ash
416 morphology on airborne tephra transport have been the subject of a great deal of
417 study, as the topic has significant implications for ash cloud modelling techniques.
418 The surface roughness, sphericity and convexity of ash particles all affect the
419 aerodynamic properties of those particles (Riley et al., 2003), which in turn affect the
420 settling velocity, atmospheric residence time, and transport distance. For example,
421 irregular particles with low vesicularities and high surface-to-volume ratios are likely
422 to aggregate due to the high wettability and surface roughness, while flat particles
423 with high long axis to short axis ratios are likely to be transported further from their
424 source (Riley et al., 2003; Cioni et al., 2014). The primary determining factors in ash
425 morphology are magma fragmentation – itself a product of gas content,
426 pressurisation and conduit width, among others – and interaction of the magma and
427 subsequent volcanic plume with water. A greater degree of interaction results in
428 greater fragmentation, giving the tephra a thinner, more concave morphology, with
429 complex implications for transport distance (Freundt & Rosi, 1998).

430 While a small number of larger ($>150\text{ }\mu\text{m}$) shards were found some samples in the
431 Stordalen and Marooned cores, the vast majority of tephra found in the Abisko
432 region has a thin, wispy morphology with an average length of 50-100 μm and pale
433 colouration, corresponding with the explosive eruptions to which all of the identified
434 ash layers have been assigned.

435

436 4.2.5 Other factors

437 An absence of water outflow is crucial to the successful preservation of a tephra
438 layer. Lakes or fens which have substantial throughflow are typically not suitable for
439 tephrochronological study, as hydrological redistribution of lighter particles is
440 substantially more likely. Dry or impermeable surfaces may also facilitate windblown
441 redistribution of tephra to topographic lows. Particles are therefore preferentially
442 preserved in low areas of damp, permeable terrain. A recent study conducted on
443 thin tephra layers in temperate regions (Blong et al., 2017) suggested that the
444 erosional reworking of tephra layers $<300\text{ mm}$ in thickness, as is the case for many
445 European cryptotephra layers, is highly variable even across relatively homogenous
446 sites. These results may indicate the necessity of large sample sizes and the
447 collection of multiple cores within small areas, although in practice this method is
448 likely to become impractical.

449

450 5 Conclusions

451 [1] Six distinct tephra layers, the majority of which are likely to be of Icelandic origin,
452 were recorded in the surveyed Abisko peatland cores.

453 [2] Using geochemical analysis, we identify shards belonging to the Hekla 4, Hekla
454 1104, Hekla 1158 and Hekla-Selsund eruptions in Abisko.

455 [3] From age-depth profiles of two cores, we suggest that the Askja 1875 tephra, and
456 an unidentified, possibly non-Icelandic tephra are present in the Abisko region.

457 [4] We find very little correlation between tephrostratigraphies of adjacent peat
458 cores, suggesting that local-scale variations in topography, vegetation, snow cover,
459 ground permeability, and other factors significantly influence the preservation of
460 windblown tephra in sub Arctic Sweden.

461 [5] The variability of tephra preservation across multiple sites within the study area
462 suggests that northern Scandinavian peatlands may be an unreliable source of
463 volcanic ash deposits due to the increased risks of redeposition and secondary
464 transport, further complicating studies into the tephrochronology of the region.

465

466 **6 Acknowledgements**

467 Claire Cooper acknowledges a Leeds Anniversary Research Scholarship at the
468 University of Leeds, in addition to support from the Climate Research Bursary Fund
469 awarded by the Priestley International Centre for Climate. Elizabeth Watson was
470 funded by NERC funded Doctoral Training Grant NE/K500847/1. We acknowledge
471 the Worldwide University Network (WUN) for funding this project (Project: Arctic
472 Environments, Vulnerabilities and Opportunities). We acknowledge the Abisko
473 Scientific Research Station for assistance with field logistics and Kallax Flyg AB for
474 helicopter support.

475

476

477

478

479

480

481

482

483

484

485

486 **Appendix A**

487 Table A.1. Radiocarbon dates of Abisko peat profiles

Site	Lab Code	Depth (cm)	¹⁴ C Age	1σ Error	Material dated	Cal range 2σ (BP)	Cal (BP)	Median	Age
Electric	UB2359	17	165	20	<i>Dicranum bergerii</i> + <i>Dicranum elongatum</i> stems with leaves	166-225	187		
	UB2360	22	390	20	<i>Sphagnum</i> stems + leaves	434-505	476		
Crater Pool I	UB2358	15	860	20	<i>Sphagnum russowii</i> stems with leaves	726-796	763		
	Poz-80223	22	1110	30	<i>Sphagnum riparium</i> stems with leaves	937-1071	1014		
Crater Pool II	UB2356	19	160	20	<i>Betula nana</i> leaf remains + fruits scale, <i>Empetrum nigrum</i> seed remains, <i>Andromeda polifolia</i> leaves and seeds, <i>Sphagnum fuscum</i> stems with leaves	167-224	187		
	UB2357	29	345	20	<i>Sphagnum fuscum</i> stems with leaves, <i>Oxycoccus palustris</i> leaves, <i>Betula nana</i> leaf remains	316-407	386		
Railway	UB2366	28	200	20	<i>Oxycoccus palustris</i> leaves, <i>Betula nana</i> leaf remains, <i>Sphagnum</i>	146-189	172		

					<i>russowii</i> stems with leaves		
	UB2398_2	40	1240	20	Bulk	1196-1263	1211
Eagle	UB2365	19	130	20	<i>Dicranum</i> <i>elongatum</i> stems with leaves, <i>Pleurozium</i> <i>schreberii</i> stems with leaves	59-149	119
	UB2397_2	30	1725	25	Bulk	1565-1700	1635
Nikka	UB2363	24	180	20	<i>Sphagnum</i> <i>fusum</i> stems with leaves	142-219	183
	UB2364	30	595	20	<i>Sphagnum</i> <i>fusum</i> stems with leaves	584-647	606
Instrument	UB2361	25	165	20	<i>Dicranum</i> <i>elongatum</i> stems with leaves	166-224	187
	UB2362	30	320	20	<i>Dicranum</i> <i>elongatum</i> stems with leaves	348-458	387
Stordalen	D-AMS 006366	14	340	24	<i>Sphagnum</i>	477-314	388
	D-AMS 006367	17	553	31	<i>Sphagnum</i>	640-518	559
Marooned	D-AMS 006368	28	2317	26	<i>Sphagnum</i> , herb epidermis	2360-2211	2342

488

489 Table A.2 ²¹⁰Pb dating of Abisko peat profiles

Site	Cumul. ²¹⁰ Pb _{ex} inventory (Bq/m ²)	±	Residual ²¹⁰ Pb _{ex} (Bq/m ²)	±	Age (year)	YEAR (AD)	±
	19.02	1.68	3632.39	26.67	0.17	2011.83	1.00
	116.57	6.13	3534.84	26.62	1.04	2010.96	1.02
	273.73	8.11	3377.68	25.96	2.50	2009.50	1.06
	504.43	11.26	3146.97	25.41	4.77	2007.23	1.08
	833.18	14.73	2818.22	24.17	8.32	2003.68	1.12
	1263.37	18.20	2388.03	22.23	13.64	1998.36	1.17
	1942.68	21.82	1708.73	19.49	24.39	1987.61	1.25
	2485.15	23.74	1166.26	15.33	36.65	1975.35	1.35
	3073.40	25.72	578.01	12.15	59.19	1952.81	1.61
	3359.58	26.35	291.83	7.05	81.14	1930.86	1.75
	3582.02	26.53	69.39	4.14	127.27	1884.73	2.89
	3651.40	26.67	0.00	2.76			
	3651.40	26.85					
Marooned	3611.87	26.91					

	3618.02	31.04					
	3556.55	33.89					
	47.57	4.29	3602.81	45.06	0.42	2011.58	1.01
	166.11	7.75	3484.27	44.85	1.50	2010.50	1.04
	553.84	18.48	3096.54	44.38	5.28	2006.72	1.10
	1239.81	25.69	2410.57	41.09	13.33	1998.67	1.25
	1923.16	30.09	1727.22	37.01	24.03	1987.97	1.43
	2521.79	40.57	1128.59	33.53	37.70	1974.30	1.71
	3064.50	43.78	585.89	19.60	58.75	1953.25	1.97
	3441.33	44.64	209.05	10.63	91.84	1920.16	2.59
	3650.38	45.06	0.00	6.09			
	3650.38	45.48					
	3606.77	45.52					
	3580.58	45.59					
	3511.91	45.65					
	3254.74	45.99					
	2968.36	47.14					
	2868.03	48.93					
Eagle	2579.98	51.08					
	129.65	12.70	2517.20	28.58	1.61	2010.39	1.02
	328.28	16.64	2318.57	25.61	4.25	2007.75	1.16
	600.43	18.59	2046.42	23.24	8.26	2003.74	1.22
	1018.88	20.87	1627.98	21.71	15.61	1996.39	1.28
	1599.29	23.67	1047.56	19.53	29.77	1982.23	1.44
	1971.58	27.37	675.27	16.03	43.87	1968.13	1.64
	2248.59	28.20	398.26	8.23	60.82	1951.18	1.65
	2455.75	28.40	191.10	4.65	84.40	1927.60	1.80
	2584.36	28.51	62.50	3.23	120.30	1891.70	2.66
	2646.85	28.58	0.00	2.05			
	2646.85	28.75					
	2618.05	29.25					
	2607.31	29.73					
	2594.90	31.04					
Nikka	2556.27	31.43					
	129.65	12.70	2517.20	28.58	1.61	2010.39	1.02
	328.28	16.64	2318.57	25.61	4.25	2007.75	1.16
	600.43	18.59	2046.42	23.24	8.26	2003.74	1.22
	1018.88	20.87	1627.98	21.71	15.61	1996.39	1.28
	1599.29	23.67	1047.56	19.53	29.77	1982.23	1.44
	1971.58	27.37	675.27	16.03	43.87	1968.13	1.64
	2248.59	28.20	398.26	8.23	60.82	1951.18	1.65
	2455.75	28.40	191.10	4.65	84.40	1927.60	1.80
	2584.36	28.51	62.50	3.23	120.30	1891.70	2.66
	2646.85	28.58	0.00	2.05			
	2646.85	28.75					
	2618.05	29.25					
	2607.31	29.73					
	2594.90	31.04					
Stordalen	2556.27	31.43					

490

491

492 **Appendix B**

493 Table B.1. Non-normalised major element glass geochemistry of Abisko peat profiles

Core	Depth (cm)	SiO ₂	TiO ₂	Al ₂ O ₃	FeO	MnO	MgO	CaO	Na ₂ O	K ₂ O	P ₂ O ₅	Total
Marooned	85	70.54	0.45	13.10	4.65	0.19	0.18	1.53	4.89	3.52	0.05	99.09
		76.16	0.24	11.91	2.06	0.08	0.07	0.90	4.19	3.03	0.03	98.69
		73.40	0.28	14.28	3.43	0.12	0.32	2.41	4.91	1.95	0.05	101.19
		71.93	0.24	13.25	2.98	0.12	-0.20	1.95	5.25	2.40	0.03	97.96
		63.12	0.85	14.63	7.49	0.23	0.89	4.45	4.17	1.87	0.28	97.98
		64.73	0.85	15.19	7.59	0.24	0.90	4.55	4.78	1.67	0.29	100.75
		73.99	0.14	12.80	2.01	0.08	0.05	1.35	5.02	2.90	0.01	98.38
		66.65	0.52	15.15	4.41	0.20	0.34	1.87	5.54	3.88	0.07	98.65
		72.96	0.13	12.14	1.94	0.09	0.03	1.18	4.67	2.82	0.00	95.98
		66.40	0.57	15.02	5.22	0.17	0.45	3.66	5.69	1.59	0.16	98.92
		66.23	0.59	15.03	4.04	0.11	0.31	3.87	5.64	1.35	0.19	97.34
		71.16	0.24	13.29	3.09	0.11	0.13	2.06	5.06	2.48	0.02	97.67
		71.96	0.23	12.95	2.84	0.11	0.10	1.87	4.71	2.58	0.02	97.41
		63.02	1.18	15.07	7.17	0.20	1.38	4.75	4.41	1.57	0.40	99.09
		64.28	1.18	14.04	7.17	0.21	1.35	4.58	4.48	1.52	0.39	99.11
		75.55	0.20	12.23	1.73	0.07	0.06	1.34	4.34	2.75	0.03	98.36
Stordalen	25	69.57	0.46	13.51	5.23	0.14	0.34	2.34	4.97	2.88	0.10	99.54
		69.36	0.42	15.53	4.17	0.11	0.19	3.01	5.34	2.44	0.10	100.68
		69.26	0.50	14.28	4.83	0.19	0.24	2.81	5.49	2.54	0.10	100.25
		68.79	0.47	15.19	5.09	0.15	0.40	3.29	5.47	2.05	0.09	100.99
		68.72	0.46	15.23	5.52	0.17	0.43	3.13	5.27	2.30	0.11	101.34
		68.68	0.47	15.41	5.46	0.17	0.47	3.15	5.12	2.32	0.10	101.35
		68.40	0.48	14.09	5.48	0.19	0.42	3.03	5.06	2.42	0.10	99.68
		68.23	0.48	14.53	5.48	0.17	0.48	3.33	5.16	2.31	0.09	100.26
		68.11	0.47	15.35	5.70	0.18	0.46	2.96	5.30	2.38	0.10	101.01
		67.90	0.47	14.36	5.31	0.18	0.44	3.14	5.54	2.30	0.11	99.75
		67.84	0.48	14.88	5.75	0.17	0.45	3.22	5.12	2.31	0.11	100.32
		67.84	0.47	14.52	5.83	0.15	0.46	3.28	4.81	2.31	0.12	99.77
		67.80	0.48	15.01	5.75	0.19	0.50	3.02	4.78	2.26	0.08	99.97
		67.66	0.46	15.06	5.70	0.18	0.46	2.94	5.71	2.24	0.09	100.51
		67.62	0.45	14.22	5.39	0.14	0.50	3.02	5.44	2.41	0.11	99.30
		67.60	0.46	14.83	5.76	0.16	0.44	3.14	5.43	2.35	0.10	100.29
		67.60	0.48	15.22	5.65	0.19	0.44	3.14	5.09	2.39	0.10	100.31
		67.39	0.46	15.04	6.06	0.17	0.46	3.02	5.55	2.30	0.11	100.56
		67.22	0.45	14.85	5.61	0.17	0.48	3.11	5.39	2.32	0.11	99.71
		67.11	0.41	16.93	4.25	0.15	0.34	3.88	5.87	1.97	0.09	101.00
		65.41	0.07	13.85	5.66	0.11	0.41	3.16	4.04	2.19	0.07	95.20
		64.71	0.27	20.15	3.10	0.07	0.31	5.19	6.36	1.32	0.06	101.54
Stordalen	30	67.63	0.38	16.11	4.01	0.16	0.26	1.78	5.73	4.18	0.05	100.29
		67.49	0.40	15.75	4.05	0.19	0.27	1.82	6.16	4.22	0.06	100.40
		67.48	0.39	16.25	4.23	0.18	0.24	1.85	6.22	4.21	0.06	101.12
		67.41	0.39	15.78	4.42	0.16	0.33	1.76	5.92	4.16	0.05	100.38
		67.28	0.47	15.85	4.69	0.19	0.46	2.05	5.97	3.94	0.09	101.01
		67.20	0.43	15.84	4.75	0.20	0.36	2.09	5.73	4.11	0.64	100.76
		66.98	0.34	15.68	3.76	0.15	0.23	1.71	6.01	4.21	0.06	99.12
		66.96	0.46	16.59	4.48	0.19	0.40	2.24	5.99	4.13	0.08	101.52
		66.76	0.43	15.94	4.34	0.16	0.37	1.98	6.14	4.07	0.06	100.25
		66.66	0.43	16.64	4.14	0.17	0.32	1.96	5.87	4.02	0.07	100.28
		66.50	0.36	16.14	4.28	0.15	0.28	1.58	6.14	4.28	0.06	99.73

66.44	0.33	14.26	3.60	0.15	0.19	1.63	5.64	4.29	0.04	96.56
66.27	0.41	15.63	4.34	0.18	0.35	1.99	6.25	4.06	0.07	99.53
65.85	0.47	14.11	5.66	0.28	0.66	2.73	5.49	4.12	0.08	99.46
65.83	0.57	16.08	5.60	0.23	0.57	2.43	5.74	3.78	0.12	100.94
65.73	0.38	15.60	4.07	0.16	0.31	1.80	5.92	4.27	0.07	98.31
65.41	0.46	15.62	4.53	0.18	0.31	1.96	6.07	3.98	0.07	98.60
65.13	0.46	15.79	4.61	0.17	0.34	2.12	6.13	3.92	0.08	98.74
64.89	0.40	15.78	4.17	0.18	0.31	1.89	5.89	4.18	0.07	97.76
63.34	0.43	15.82	4.25	0.16	0.31	1.87	5.71	3.95	0.06	95.91

Marooned	70	72.02	0.62	14.51	2.45	0.16	0.53	1.71	6.08	2.84	0.10	100.96
		64.63	0.77	15.68	5.58	0.24	0.54	2.65	6.43	3.65	0.16	100.27
		72.73	0.64	13.28	3.17	0.15	0.69	2.61	4.65	1.71	0.13	99.73
		71.16	0.25	13.54	3.02	0.12	0.12	1.98	4.66	2.36	0.03	97.28
		70.33	0.31	13.18	3.82	0.17	0.11	1.29	4.87	5.10	0.04	99.24
		65.73	0.67	14.49	6.32	0.21	0.58	3.43	4.99	1.95	0.20	98.55
		71.67	0.25	13.34	3.00	0.12	0.13	1.85	5.08	2.42	0.02	97.90
		71.40	0.23	13.42	2.98	0.14	0.02	1.79	5.64	2.78	0.01	98.42
		64.60	0.77	14.05	7.17	0.23	0.78	3.93	4.40	1.67	0.24	97.82
		72.28	0.24	13.55	3.13	0.12	0.11	1.92	5.84	2.42	0.03	99.63

494

495 Table B.2 EMPA of Lipari and BCR-2G glass standards prior to Abisko glass shard

496 analysis

DataSet	SiO2	TiO2	Al2O3	FeO	MnO	MgO	CaO	Na2O	K2O	P2O5	Total	Comment	Mean Z
1 / 1 .	55.20	2.30	13.56	12.15	0.20	3.60	6.93	3.21	1.79	0.36	99.29	BCR2g	12.7
2 / 1 .	54.41	2.26	13.38	12.48	0.17	3.72	7.13	3.28	1.74	0.38	98.96	BCR2g	12.7
3 / 1 .	54.54	2.26	13.16	12.58	0.21	3.75	6.91	3.32	1.88	0.39	99.00	BCR2g	12.7
4 / 1 .	53.96	2.26	13.23	12.38	0.20	3.77	7.03	3.52	1.79	0.38	98.51	BCR2g	12.6
5 / 1 .	74.43	0.07	12.70	1.76	0.07	0.04	0.81	4.18	5.23	0.00	99.30	Lipari	11.2
6 / 1 .	74.04	0.08	12.68	1.63	0.07	0.04	0.71	4.16	4.96	0.01	98.36	Lipari	11.1
7 / 1 .	74.78	0.07	12.99	1.59	0.07	0.06	0.72	4.27	5.21	0.00	99.76	Lipari	11.2
8 / 1 .	74.50	0.07	12.80	1.65	0.07	0.02	0.79	4.01	5.24	0.00	99.15	Lipari	11.2
9 / 1 .	54.11	2.26	13.23	12.50	0.18	3.69	6.99	3.21	1.86	0.36	98.40	BCR2g	12.6
10 / 1 .	54.70	2.27	13.33	12.72	0.20	3.76	7.09	3.42	1.76	0.36	99.60	BCR2g	12.8
11 / 1 .	54.92	2.26	13.41	12.62	0.19	3.66	7.11	3.42	1.81	0.38	99.77	BCR2g	12.8
12 / 1 .	54.22	2.28	13.08	11.70	0.20	3.80	7.00	3.25	1.86	0.35	97.74	BCR2g	12.4

497

498 Appendix C

499 Table C.1 Site information

Site name	Codes	Latitude (°N)	Longitude (°E)	Peatland type	Number of samples	Water table depth range (cm)	pH range
Craterpool	P1-7	68°19'10.1"	19°51'27.2"	Palsa	7	- 5 to 45	3.76–4.77
Eagle	E1-6	68°21'56.5"	19°35'02.9"	Fen and bog	6	0 to 29	4.52–6.74
Electric	L1-6	67°51'56.1"	19°22'06.4"	Palsa	6	0 to 45	3.66–6.95

Site name	Codes	Latitude (°N)	Longitude (°E)	Peatland type	Number of samples	Water table depth range (cm)	pH range
Instrument	I1-6	68°11'52.4"	19°45'56.2"	Palsa	6	0 to 36	3.43–5.32
Marooned	M1-7	67°57'24.0"	19°59'11.4"	Fen and bog	7	– 1 to 29	3.24–4.21
Nikka	N1-6	67°52'02.2"	19°10'42.5"	Fen and bog	6	– 1 to 40	4.02–5.27
Railway	R1-7	68°05'12.6"	19°49'52.9"	Palsa	7	0 to 40	3.25–6.35
Stordalen	S1-40	68°21'24.3"	19°02'53.5"	Palsa and fen	40	– 7 to 50	2.99–3.80

500

501 References

- 502 1. Alatalo, J.M., Jägerbrand, A.K. and Molau, U. 2016. Impacts of different
503 climate change regimes and extreme climatic events on an alpine meadow
504 community. *Scientific Reports*, 6 (21720)
- 505 2. Alfano, F., Bonadonna, C., Volentik, A.C., Connor, C.B., Watt, S.F., Pyle, D.M.
506 and Connor, L.J., 2011. Tephra stratigraphy and eruptive volume of the May,
507 2008, Chaitén eruption, Chile. *Bulletin of Volcanology*, 73(5), pp.613-630.
- 508 3. Appleby, P. G. 2001. Chronostratigraphic techniques in recent sediments *in*
509 *Tracking environmental change using lake sediments Vol. 2: Physical and*
510 *geochemical methods* (eds Last, W. M. & Smol, J. P.) 171–203. Springer.
- 511 4. Bergman, J., Wastegård, S., Hammarlund, D., Wohlfarth, B. and Roberts, S. J.
512 2004. Holocene tephra horizons at Klocka Bog, west-central Sweden: aspects
513 of reproducibility in subarctic peat deposits. *J. Quaternary Sci.*, 19: 241–249.
514 doi:10.1002/jqs.833
- 515 5. Blockley, S.P.E. et al. 2005. A new and less destructive laboratory procedure
516 for the physical separation of distal glass tephra shards from sediments.
517 *Quat. Sci. Rev.*, 24, pp. 1952-1960
- 518 6. Blong, R., Enright, N., and Grasso, P. 2017. Preservation of thin tephra.
519 *Journal of Applied Volcanology*, 6. [https://doi.org/10.1186/s13617-017-0059-](https://doi.org/10.1186/s13617-017-0059-4)
520 4
- 521 7. Bourne, A.J., Abbott, P.M., Albert, P.G., Cook, E., Pearce, N.J., Ponomareva,
522 V., Svensson, A. and Davies, S.M., 2016. Underestimated risks of recurrent

523 long-range ash dispersal from northern Pacific Arc volcanoes. Scientific
524 Reports, 629837.

525 8. Cadle, R.D., Kiang, C.S. and Louis, J.-F. 1976. The global scale dispersion of the
526 eruption clouds from major volcanic eruptions. *Journal of Geophysical*
527 *Research*, 81, 3125-3132

528 9. Callaghan, T.V., Bergholm, F., Christensen, T.R., Jonasson, C., Kokfelt, U.,
529 Johansson, M., 2010. A new climate era in the sub-Arctic: Accelerating
530 climate changes and multiple impacts. *Geophys Res Lett* 37, 14705.

531 10. Camill, P. 1999. Patterns of boreal permafrost peatland vegetation across
532 environmental gradients sensitive to climate warming. *Canadian Journal of*
533 *Botany*, 77 (5), 721-733

534 11. Camill, P. 2004. Permafrost thaw accelerates in boreal peatlands during late-
535 20th century climate warming. *Climatic Change*, 68 (1-2), 135-152

536 12. Cioni, R. et al. 2014. Insights into the dynamics and evolution of the 2010
537 Eyjafjallajökull summit eruption (Iceland) provided by volcanic ash textures.
538 *Earth and Planetary Science Letters*, 394, 111-123

539 13. Cutler, N.A., Bailey, R.M., Hickson, K.T., Streeter, R.T., and Dugmore, A.J.,
540 2016. Vegetation structure influences the retention of airfall tephra in a sub-
541 Arctic landscape. *Progress in Physical Geography: Earth and Environment* , 40
542 (5), 661-675

543 14. Davies, S.M. et al. 2010. Widespread dispersal of Icelandic tephra: how does
544 the Eyjafjöll eruption of 2010 compare to past Icelandic events? *Journal of*
545 *Quaternary Science: Rapid Communication*, 25 (5), 605-611

546 15. Dugmore, A. J., and Newton, A. J. 1992. Thin tephra layers in peat revealed by
547 X-radiography. *J. Archaeol. Sci.*, 19, 163–170, doi:10.1016/0305-
548 4403(92)90047-7.

549 16. Dugmore, A., Streeter, R. and Cutler, N. 2018. The role of vegetation cover
550 and slope angle in tephra layer preservation and implications for Quaternary
551 tephrostratigraphy. *Palaeogeography, Palaeoclimatology, Palaeoecology*,
552 489, 105-116

553 17. Durant, A.J., Villarosa, G., Rose, W.I., Delmelle, P., Prata, A.J. and Viramonte,
554 J.G., 2012. Long-range volcanic ash transport and fallout during the 2008

- eruption of Chaitén volcano, Chile. *Physics and Chemistry of the Earth, Parts A/B/C*, 45, 50-64.
18. Freundt, A. and Rosi, M. 1998. *From magma to tephra : modelling physical processes of explosive volcanic eruptions*. 1st ed. Elsevier, Published Amsterdam ; New York. ISBN: 0444829598
19. Gałka, M. et al. 2017. Vegetation Succession, Carbon Accumulation and Hydrological Change in Subarctic Peatlands, Abisko, Northern Sweden. *Permafrost and Periglac. Process.*, 28, 589-604. doi: [10.1002/ppp.1945](https://doi.org/10.1002/ppp.1945).
20. Global Volcanism Program, 1998. Report on Grimsvotn (Iceland). In Wunderman, R (ed.), *Bulletin of the Global Volcanism Network*, 23:11. Smithsonian Institution. <https://dx.doi.org/10.5479/si.GVP.BGVN199811-373010>.
21. Global Volcanism Program, 2000. Report on Hekla (Iceland). In Wunderman, R (ed.), *Bulletin of the Global Volcanism Network*, 25:2. Smithsonian Institution. <https://dx.doi.org/10.5479/si.GVP.BGVN200002-372070>.
22. Global Volcanism Program, 2013. Krafla (373080) In *Volcanoes of the World*, v. 4.6.6. Venzke, E (ed.). Smithsonian Institution. Downloaded 16 Feb 2018 (<http://volcano.si.edu/volcano.cfm?vn=373080>). <https://dx.doi.org/10.5479/si.GVP.VOTW4-2013>
23. Gronvold, K. and Jóhannesson, H., 1984. Eruption in Grímsvötn 1983; course of events and chemical studies of the tephra. *Jökull*, (34), 1-8.
24. Hayward, C., 2012. High spatial resolution electron probe microanalysis of tephra and melt inclusions without beam-induced chemical modification. *The Holocene* 22, 119-125.
25. Kim, B.-M. et al. 2014. Weakening of the stratospheric polar vortex by Arctic sea-ice loss. *Nature Communications*, 5 (4646) doi:10.1038/ncomms5646
26. Lacasse, C. 2001. Influence of climate variability on the atmospheric transport of Icelandic tephra in the subpolar North Atlantic. *Global and Planetary Change*, 29 (1-2), 31-55
27. Lai, D.Y.F., 2009. Methane dynamics in northern peatlands: a review. *Pedosphere*, 19(4), 409-421.

- 587 28. Lane, C.S., Cullen, V.L., White, D., Bramham-Law, C.W.F. and Smith, V.C. 2014.
588 Cryptotephra as a dating and correlation tool in archaeology. *Journal of*
589 *Archaeological Science*, 42, 42-50
- 590 29. Lane, C.S., Lowe, D.J., Blockley, S.P.E., Suzuki, T. and Smith, V.C. 2017.
591 Advancing tephrochronology as a global dating tool: Applications in
592 volcanology, archaeology and palaeoclimatic research. *Quaternary*
593 *Geochronology*, 40, 1-7
- 594 30. Larsen, G . 1993 . Nokkur orð um Kötlugjósku. In Larsen, G., ed. *Kötlustefna*,
595 March 27-29, ágrip erinda (abstracts). Reykjavík , Raunvisindastofnun, 6- 7.
596 (Háskólans Fjölrit RH-3-93.)
- 597 31. Lett, S. 2017. Mosses as mediators of climate change: implications for tree
598 seedling establishment in the tundra. Doctoral thesis, Umeå University
- 599 32. Lowe, D.J. 2011. Tephrochronology and its application: A review. *Quaternary*
600 *Geochronology*, 6(2), 107-153
- 601 33. Lundin, E.J. et al. 2016. Is the subarctic landscape still a carbon sink? Evidence
602 from a detailed catchment balance. *Geophysical Research Letters*, 43 (5),
603 1988-1995
- 604 34. Mairs, K.A., Church, M.J., Dugmore, A.J., Sveinbjarnardóttir, G., Arneborg, J.,
605 and Grønnow, B. 2006. Degrees of success: evaluating the environmental
606 impacts of successful long term settlement in south Iceland. In *The Dynamics*
607 *of Northern Societies*. PNM, Publications from the National Museum, Studies
608 in Archaeology and History, 10, 363-372. ISBN: 87-7602-052-5
- 609 35. Osterkamp, T.E. and Romanovsky, V.E. 1999. Evidence for warming and
610 thawing of discontinuous permafrost in Alaska. *Permafrost and Periglacial*
611 *Processes*, 10 (1), 17-37
- 612 36. Palais, J.M., Germani, M.S. and Zielinski, G.A. 1992. Inter-hemispheric
613 transport of volcanic ash from a 1259 A.D. volcanic eruption to the Greenland
614 and Antarctic ice sheets. *Geophysical Research Letters*, 19 (8), 801-804
- 615 37. Pilcher, J.R. and Hall, V.A. 1996. Tephrochronological studies in northern
616 England. *The Holocene*, 6 (1), 100-105.

- 617 38. Pilcher, J., Bradley, R.S., Francus, P. and Anderson, L., 2005. A Holocene
618 tephra record from the Lofoten Islands, arctic Norway. *Boreas*, 34(2), pp.136-
619 156.
- 620 39. Plunkett, G. and Pilcher, J. 2018. Defining the potential source region of
621 volcanic ash in northwest Europe during the Mid- to Late Holocene. *Earth*
622 *Science Reviews*, 179, 20-37
- 623 40. Ravikumar, S., Surekha, R., Thavarajah, R. 2014. Mounting media: An
624 overview. *J. NTR. Univ. Health Sci.*, 3, Suppl S1:1-8
- 625 41. Reimer, P.J., et al., 2013. IntCal13 and Marine13 radiocarbon age calibration
626 curves 0–50,000 years cal BP. *Radiocarbon*, 55(4), pp.1869-1887.
- 627 42. Riley, C. M., Rose, W. I., and Bluth, G. J. S. 2003. Quantitative shape
628 measurements of distal volcanic ash. *J. Geophys. Res.*, 108, 2504,
629 doi:10.1029/2001JB000818, B10.
- 630 43. Rose, W.I. and Durant, A.J., 2009. Fine ash content of explosive
631 eruptions. *Journal of Volcanology and Geothermal Research*, 186(1-2), 32-39.
- 632 44. Salmi, M. 1948. The Hekla ash falls in Finland. *Suomen Geologinen Seura* 21:
633 87–96.
- 634 45. Schuur, E.A.G. and Abbott, B. 2011. Climate change: High risk of permafrost
635 thaw. *Nature*, 480, 32-33
- 636 46. Sigurdsson, H., and Sparks, R.S.J., 1981. Petrology of rhyolitic and mixed
637 magma ejecta from the 1875 eruption of Askja, Iceland. *Journal of Petrology*,
638 22(1), 41-84.
- 639 47. Stevenson, J.A., et al. 2012. Distal deposition of tephra from the
640 Eyjafjallajökull 2010 summit eruption. *Journal of Geophysical Research: Solid*
641 *Earth*, 117(B9).
- 642 48. Stivrins N., Wulf S., Wastegard S., Lind E.M., Alliksaar T., Gałka M., Andersen
643 T.J., Heinsalu A., Seppa H., Veski S., 2016. Detection of the Askja AD 1875
644 cryptotephra in Latvia, Eastern Europe. *Journal of Quaternary Science*, 31,
645 437-441.
- 646 49. Swindles, G.T., De Vleeschouwer F. and Plunkett, G. 2010. Dating peat
647 profiles using tephra: stratigraphy, geochemistry and chronology. *Mires and*
648 *Peat*, 7 (5), 1-9

- 649 50. Swindles, G.T., Lawson, I.T., Savov, I.P., Connor, C.B. and Plunkett, G. 2011. A
650 7000 yr perspective on volcanic ash clouds affecting northern Europe.
651 *Geology*, 39, 887-890
- 652 51. Swindles, G.T. et al. 2015a. Evaluating the use of testate amoebae for
653 palaeohydrological reconstruction in permafrost peatlands. *Palaeogeography*,
654 *Palaeoclimatology*, *Palaeoecology*, 424, 111-122.
655 <https://doi.org/10.1016/j.palaeo.2015.02.004>
- 656 52. Swindles, G.T., et al. 2015b. The long-term fate of permafrost peatlands
657 under rapid climate warming. *Scientific Reports* 5, 17951.
- 658 53. Swindles, G.T., Watson, E.J., Savov, I.P., Cooper, C.L., Lawson, I.T., Schmidt, A.
659 and Carrivick, J.L. 2017. Holocene volcanic ash database for Northern Europe.
660 Database. DOI: 10.13140/RG.2.2.11395.60966
- 661 54. Swindles, G.T., et al. 2018. Climatic control on Icelandic volcanic activity
662 during the mid-Holocene. *Geology*, 46, 47-50
- 663 55. Thorarinsson, S. 1967. The eruptions of Hekla in historical times: A
664 tephrochronological study. In *The Eruption of Hekla 1947-1948*, Einarsson T,
665 Kjartansson G, Thorarinsson S (eds). *Societas Scientiarum Islandica: Reykjavik*;
666 1-170.
- 667 56. Vikhamer-Schuler, D., Isaksen, K., Haugen, J.E. and Tømmervik, H. 2016.
668 Changes in Winter Warming Events in the Nordic Arctic Region. *Journal of*
669 *Climate*, 29 (17), 6223-6244
- 670 57. Wastegård, S., Rundgren, M., Schoning, K., Andersson, S., Björck, S.,
671 Borgmark, A. and Possnert, G., 2008. Age, geochemistry and distribution of
672 the mid-Holocene Hekla-S/Kebister tephra. *The Holocene*, 18(4), 539-549.
- 673 58. Watson, E.J., Swindles, G.T., Lawson, I.T. and Savov, I.P. 2015. Spatial
674 variability of tephra and carbon accumulation in a Holocene peatland.
675 *Quaternary Science Reviews*, 124, 248-264
- 676 59. Watson, E.J., Swindles, G.T., Lawson, I.T. and Savov, I.P. 2016a. Do peatlands
677 or lakes provide the most comprehensive distal tephra records? *Quaternary*
678 *Science Reviews*, 139, 110-128
- 679 60. Watson, E.J., Swindles, G.T., Stevenson, J.A., Savov, I. and Lawson, I.T. 2016b.
680 The transport of Icelandic volcanic ash: Insights from northern European

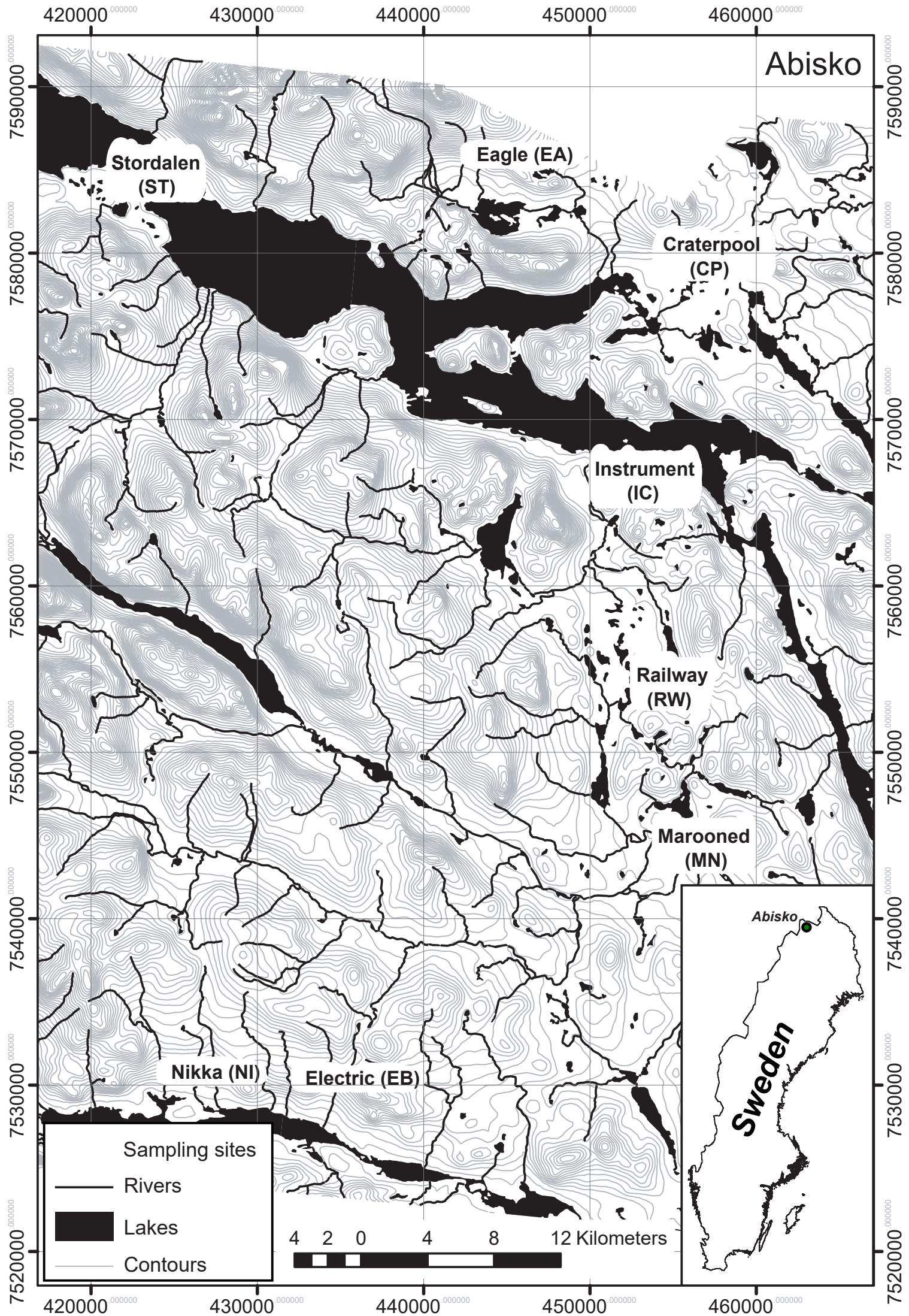
cryptotephra records. Journal of Geophysical Research: Solid Earth, 121(10),
7177-7192

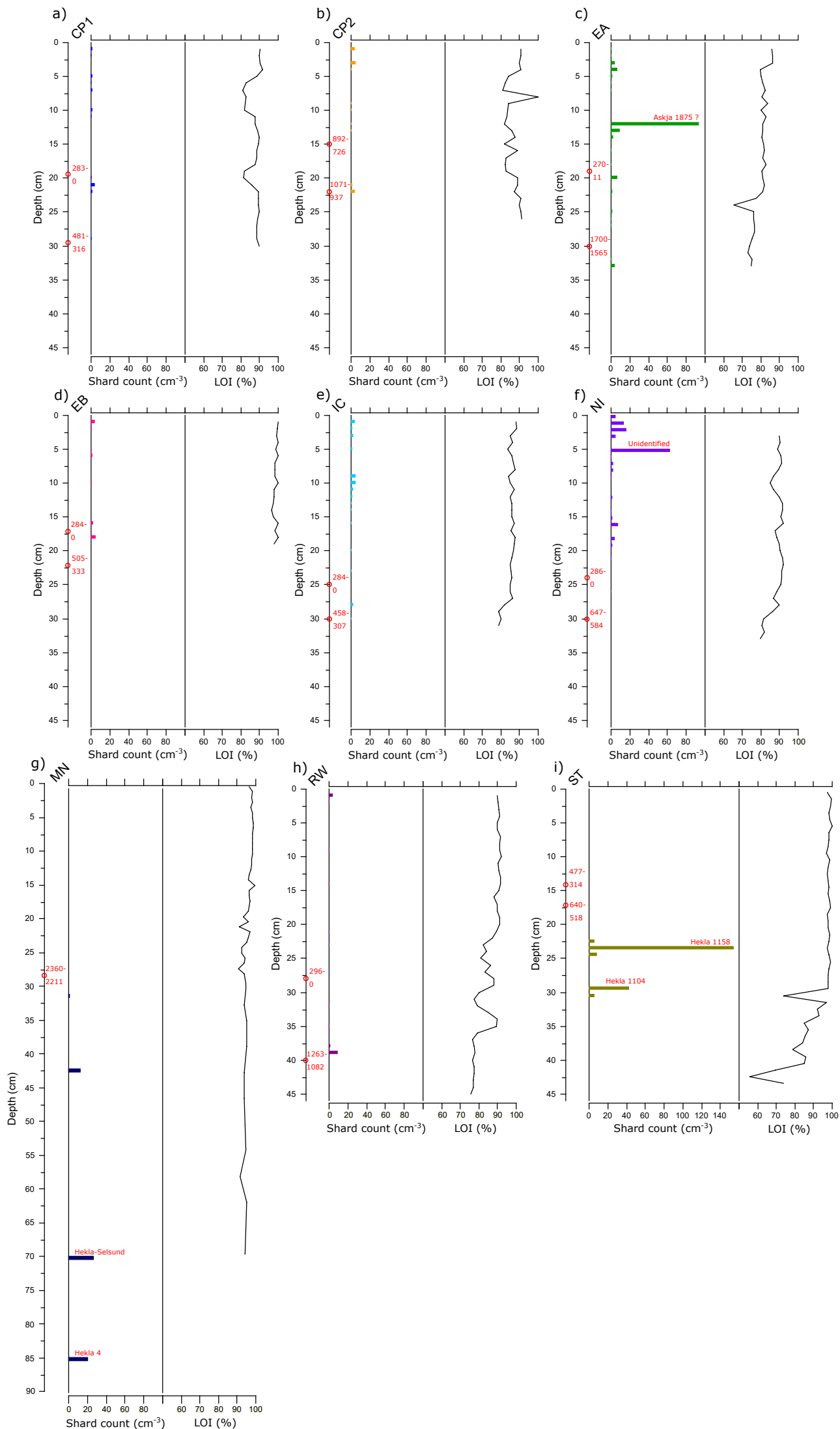
61. Watson, E.J., Swindles, G.T., Savov, I., Lawson, I.T., Connor, C. and Wilson, J.
2017. [Estimating the frequency of volcanic ash clouds over northern
Europe](#). Earth and Planetary Science Letters 460, 41-49.

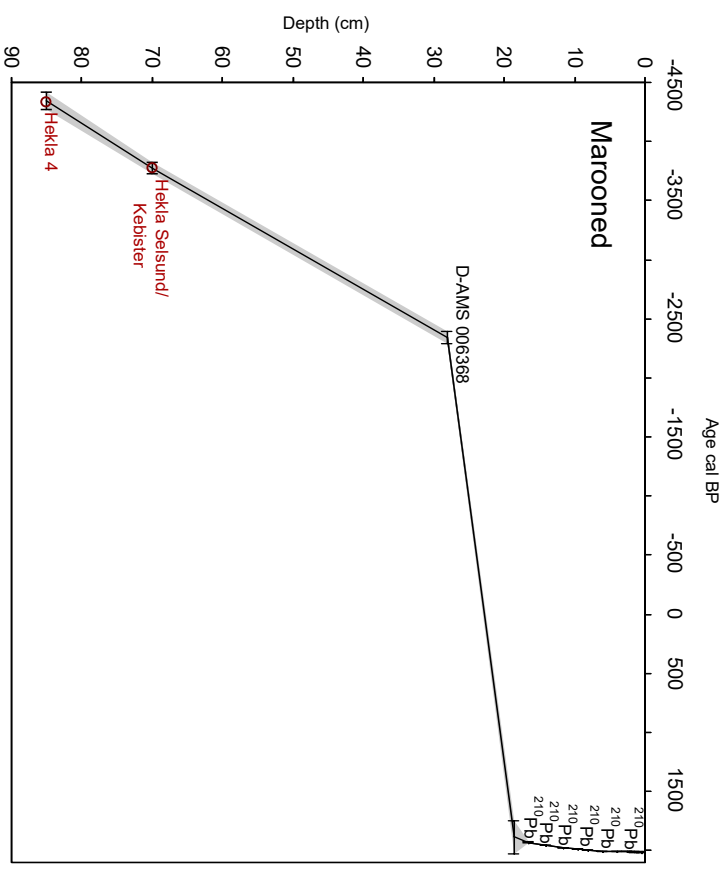
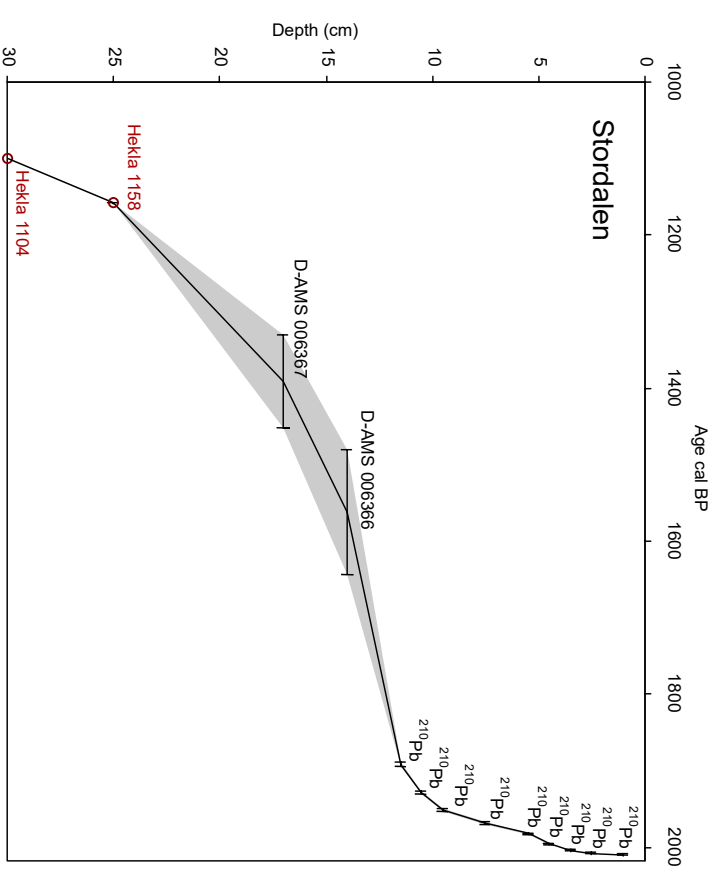
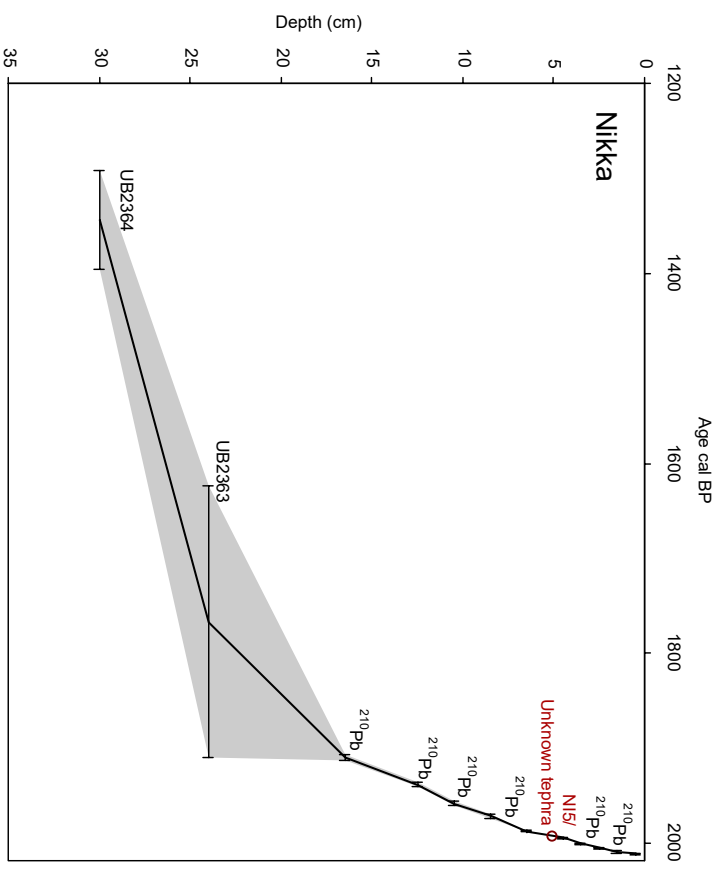
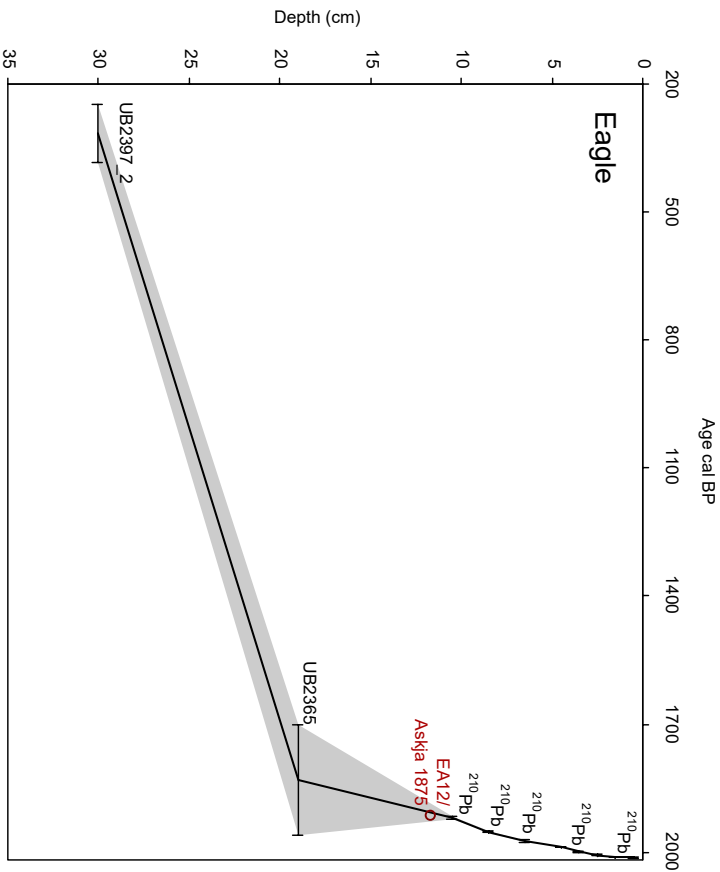
62. Watt, S.F., Pyle, D.M., Mather, T.A., Martin, R.S. and Matthews, N.E., 2009.
Fallout and distribution of volcanic ash over Argentina following the May
2008 explosive eruption of Chaitén, Chile. Journal of Geophysical Research:
Solid Earth, 114(B4).

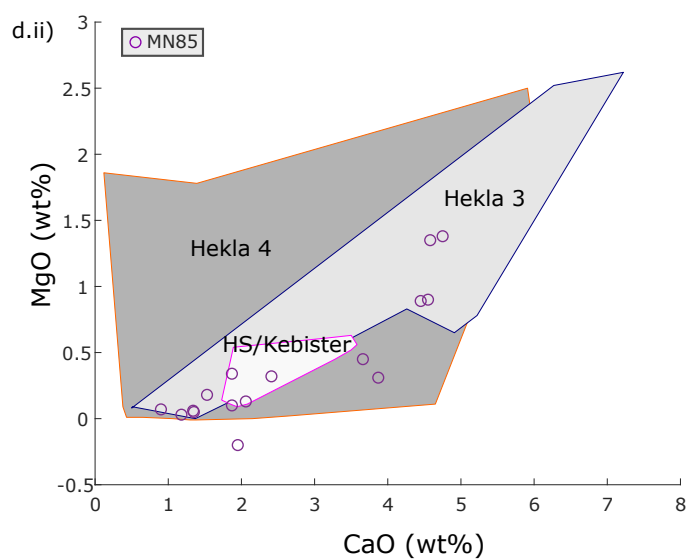
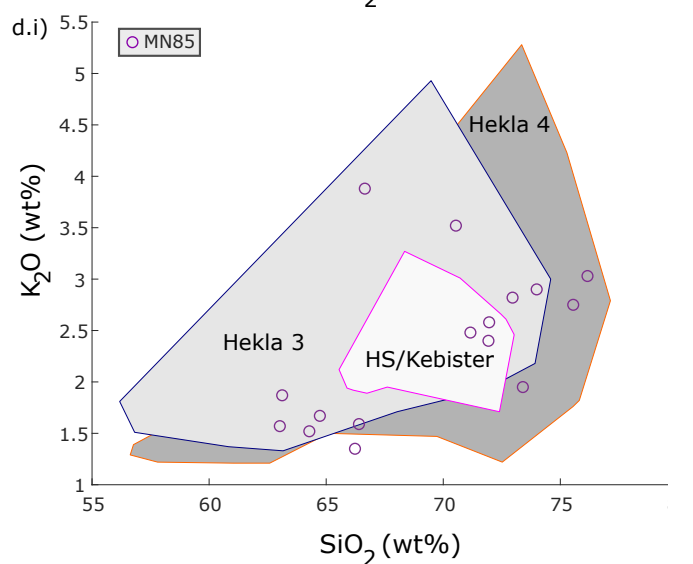
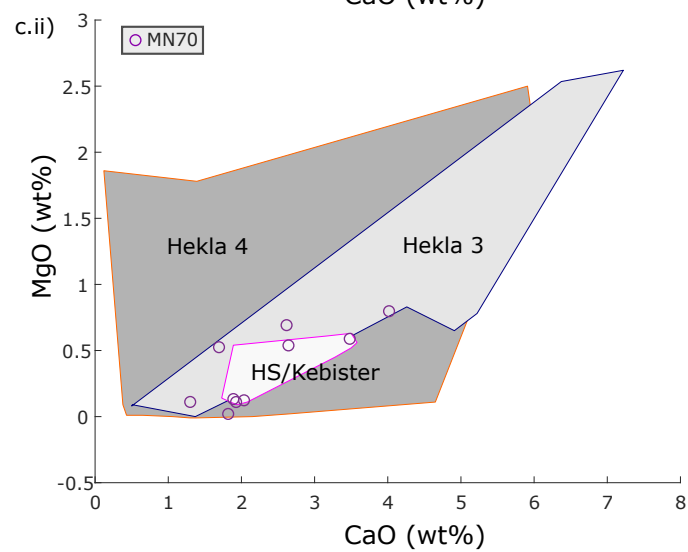
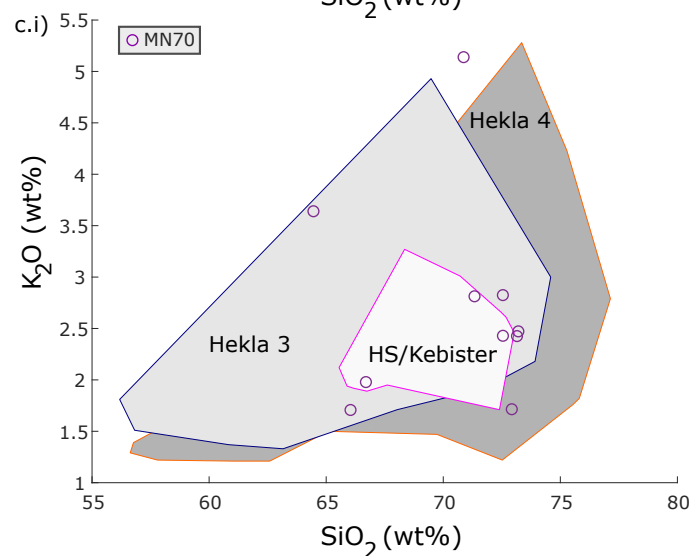
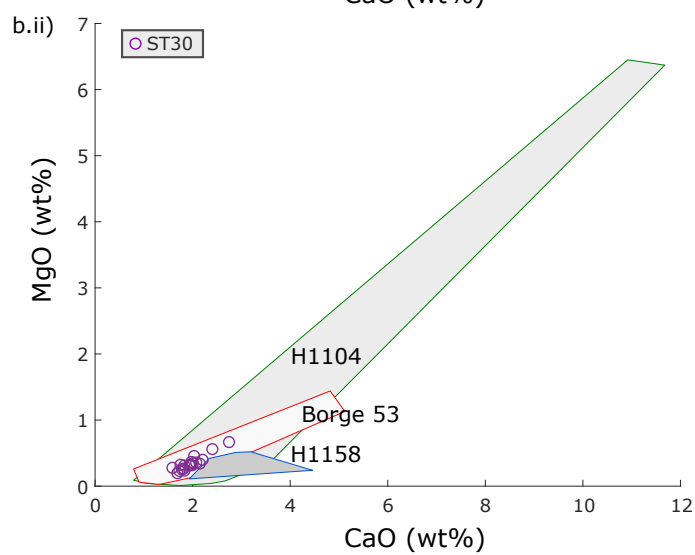
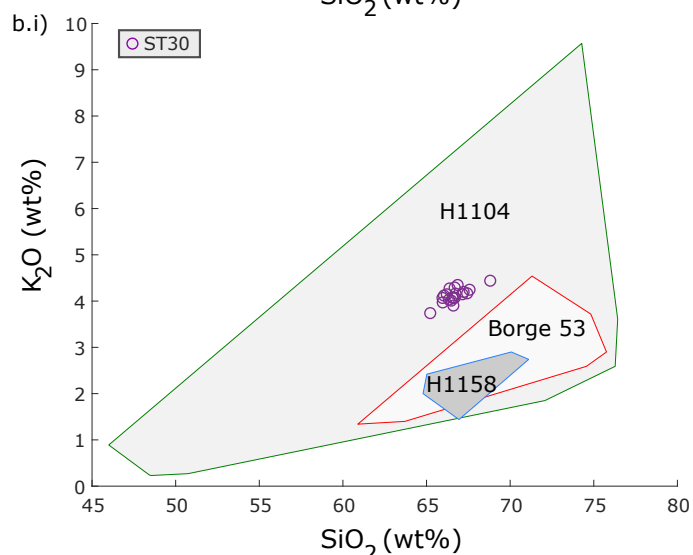
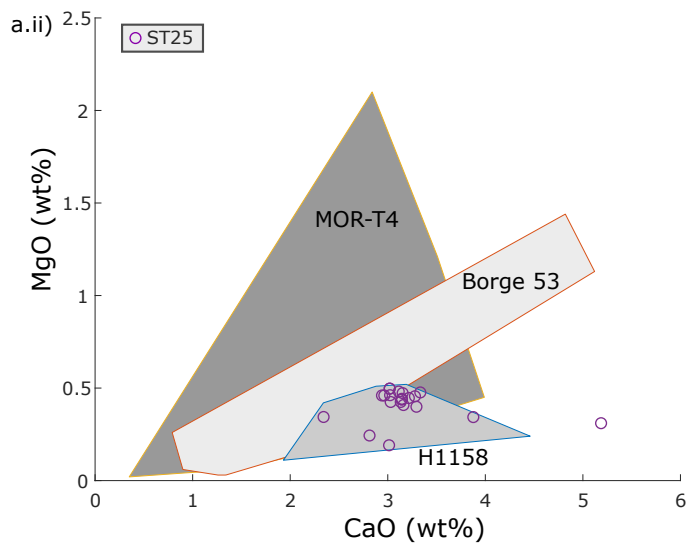
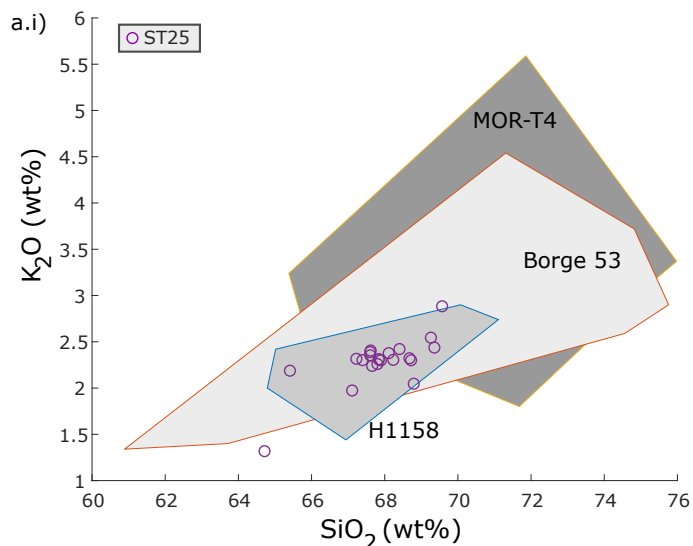
63. Whittle, A. and Gallego-Sala, A.V. 2016. Vulnerability of the peatland carbon
sink to sea level rise. Scientific Reports, 6, 28758.

64. Woollings, T., Hannachi, A. and Hoskins, B. 2010. Variability of the North
Atlantic eddy-driven jet stream. Quarterly Journal of the Royal
Meteorological Society, 136 (649), 856-868

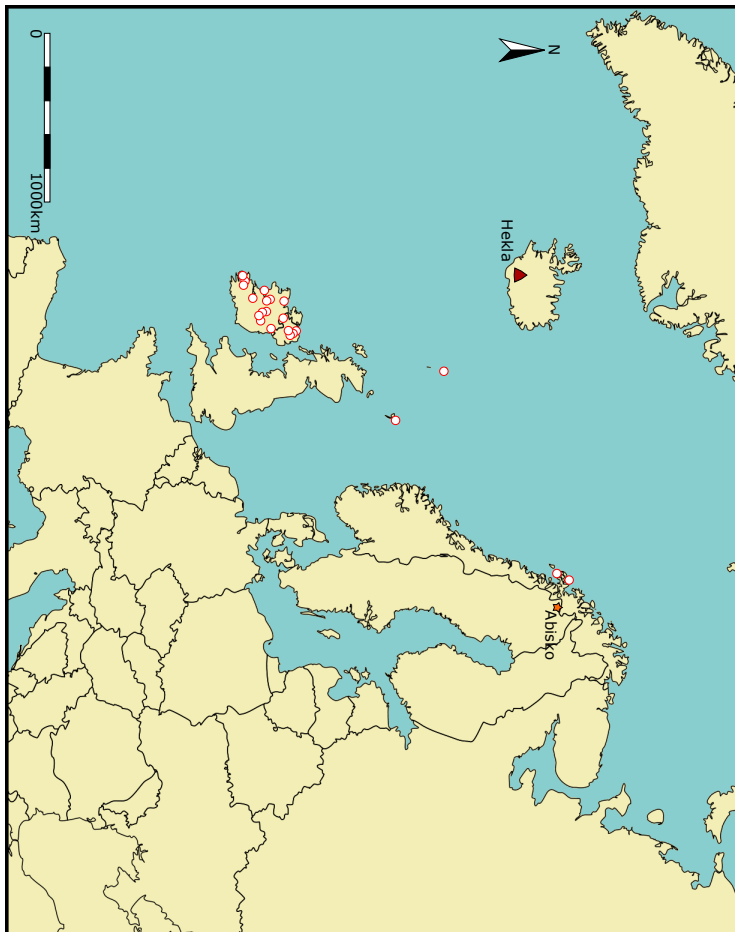




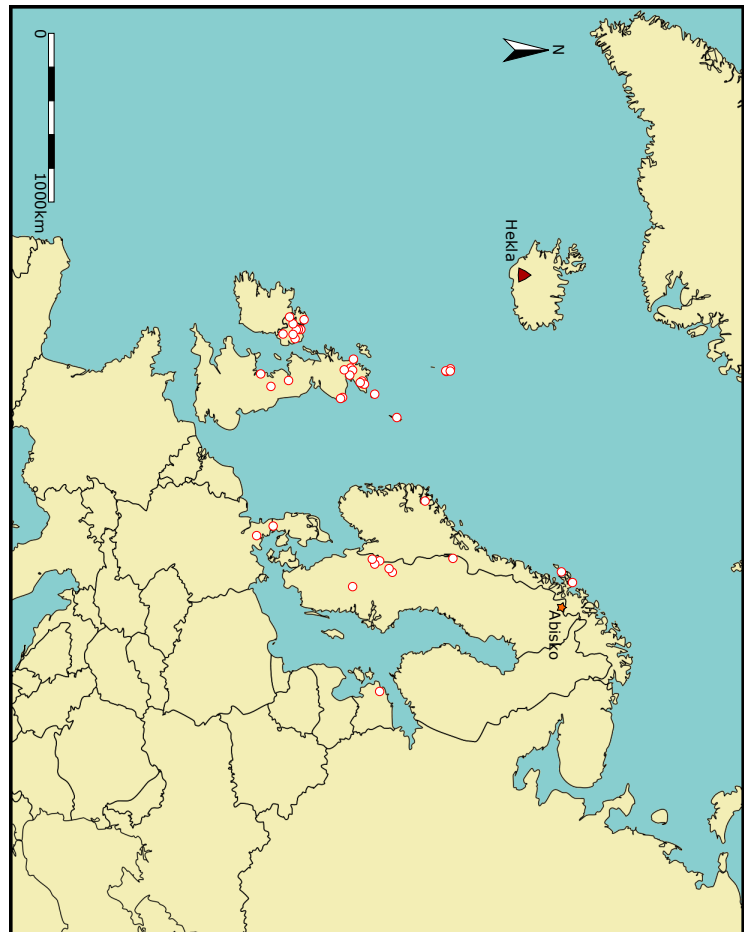




Hekla 1104



Hekla 4



Hekla 1158



Hekla S/Kebister



